



HAL
open science

Novel nanocomposite concept based on crosslinking of hyperbranched polymers in reactive cellulose nanopaper templates

Marielle Henriksson, Linda Fogelström, Lars A. Berglund, Mats Johansson, Anders Hult

► To cite this version:

Marielle Henriksson, Linda Fogelström, Lars A. Berglund, Mats Johansson, Anders Hult. Novel nanocomposite concept based on crosslinking of hyperbranched polymers in reactive cellulose nanopaper templates. *Composites Science and Technology*, 2010, 71 (1), pp.13. 10.1016/j.compscitech.2010.09.006 . hal-00702323

HAL Id: hal-00702323

<https://hal.science/hal-00702323>

Submitted on 30 May 2012

HAL is a multi-disciplinary open access archive for the deposit and dissemination of scientific research documents, whether they are published or not. The documents may come from teaching and research institutions in France or abroad, or from public or private research centers.

L'archive ouverte pluridisciplinaire **HAL**, est destinée au dépôt et à la diffusion de documents scientifiques de niveau recherche, publiés ou non, émanant des établissements d'enseignement et de recherche français ou étrangers, des laboratoires publics ou privés.

Accepted Manuscript

Novel nanocomposite concept based on crosslinking of hyperbranched polymers in reactive cellulose nanopaper templates

Marielle Henriksson, Linda Fogelström, Lars A. Berglund, Mats Johansson, Anders Hult

PII: S0266-3538(10)00351-9
DOI: [10.1016/j.compscitech.2010.09.006](https://doi.org/10.1016/j.compscitech.2010.09.006)
Reference: CSTE 4809

To appear in: *Composites Science and Technology*

Received Date: 9 April 2010
Revised Date: 7 September 2010
Accepted Date: 13 September 2010

Please cite this article as: Henriksson, M., Fogelström, L., Berglund, L.A., Johansson, M., Hult, A., Novel nanocomposite concept based on crosslinking of hyperbranched polymers in reactive cellulose nanopaper templates, *Composites Science and Technology* (2010), doi: [10.1016/j.compscitech.2010.09.006](https://doi.org/10.1016/j.compscitech.2010.09.006)

This is a PDF file of an unedited manuscript that has been accepted for publication. As a service to our customers we are providing this early version of the manuscript. The manuscript will undergo copyediting, typesetting, and review of the resulting proof before it is published in its final form. Please note that during the production process errors may be discovered which could affect the content, and all legal disclaimers that apply to the journal pertain.



Novel nanocomposite concept based on crosslinking of hyperbranched polymers in reactive cellulose nanopaper templates

Marielle Henriksson^{1~}, Linda Fogelström^{1~}, Lars A. Berglund^{1,2*}, Mats Johansson^{1,2},
Anders Hult^{1,2}

¹Fibre and Polymer Technology, Royal Institute of Technology, KTH, SE-100 44
Stockholm, Sweden

²Wallenberg Wood Science Center, Royal Institute of Technology, KTH, SE-100 44
Stockholm, Sweden

* Corresponding author: phone: +46-8-7908118; fax: +46-8-7908101; e-mail:

blund@kth.se

~ These authors contributed equally to this work.

Abstract

Cellulosic fibers offer interesting possibilities for good interfacial adhesion due to the high density of hydroxyl groups at the surface. In the present study, the potential of a new nanocomposite concept is investigated, where a porous cellulose nanofiber network is impregnated with a solution of reactive hyperbranched polyester. The polymer is chemically cross-linked to form a solid matrix. The resulting nanocomposite structure is unique. The matrix surrounds a tough nanopaper structure consisting of approximately 20 nm diameter nanofibers with an average interfiber distance of only about 6 nm. The cross-linked polymer matrix shows strongly altered characteristics when it is cross-linked in the confined space within the nanofiber network, including dramatically increased T_g, and this must be due to covalent matrix-nanofiber linkages.

Keywords: A. Nano composites, B. Fibre/matrix bond, B. Interface, D. Dynamic mechanical thermal analysis (DMTA), Cellulose nanofiber.

Introduction

Cellulose nanocomposites attract great interest. In the present paper, we add to their potential by utilizing a highly functional hyperbranched polymer matrix system in a cellulose nanopaper structure. The highly functional hyperbranched prepolymers, in combination with the large specific surface area of the hydroxyl-functional cellulose network, creates unprecedented nanofiber-matrix interaction. This adds a new synergistic characteristic to the well-known cellulose advantages. Cellulose is obtained from renewable resources, is of low cost, has high crystal modulus [1] and potentially high tensile strength [2]. An important characteristic is the network-forming ability of cellulose nanofibers [3,4]. In addition to strong reinforcement effects on mechanical properties of polymers [5,6], cellulose nanofibers strongly increase the thermal stability [3,4], decrease the thermal expansion [7], and improve the thermal conductivity [8] of the polymer matrix. Transparent composites can be obtained due to the nanoscale of cellulose nanofibers [7,9]. In the context of clear polymer coatings, nanocellulose reinforcement has the potential to preserve transparency and at the same time strongly improve mechanical properties.

In a previous study, an enzymatic pretreatment procedure was developed in order to facilitate preparation of cellulose nanofibers from wood pulp [10,11]. These nanofibers were used as composite-material reinforcement [12], and as cell wall reinforcement in polymer foams [13]. Recently, we reported on high mechanical performance of cellulose nanopaper structures [14] and related nanocomposites with a

plasticized starch matrix [15]. It is important to investigate new types of polymer matrices for cellulose nanocomposites to extend their property range.

Polymer latexes and water-soluble polymers are the most commonly used matrices [5,6], since they are conveniently combined with cellulose nanofibers dispersed in water. Polymerization routes are also interesting to explore. In the search for reactive monomers and prepolymers, processing criteria are critical. Since the present composites are prepared by impregnation of a nanofiber network, low viscosity is required for complete impregnation. The use of phenol formaldehyde of low molar mass [16], melamine formaldehyde [12], acrylates and epoxies [7] has been reported. In the present study, a hyperbranched polymer is used since it has potential as a member of a new class of reactive matrix-forming molecules in nanofiber networks.

Hyperbranched polymers have a highly branched structure with a large number of end-groups [17,18]. Consequently, the structure is usually globular with a high density of functional groups at the surface. The compact conformation leads to low viscosity and Newtonian rheology [19]. During cross-linking, the kinetics can be very fast due to the high accessibility of functional groups. The resulting polymer network has a structure largely predetermined by the hyperbranched polymer. This is highly versatile since the center can have certain structural characteristics, whereas the surface functionality can be tailored to provide specific reactions or solubility properties. The globular structure precludes the entanglement mechanisms that linear polymers are subjected to, and enables the hyperbranched polymer to easily flow into the web of cellulose nanofibers, even at comparatively high molecular weights.

In the present study we investigate the potential of a new nanocomposite concept, where porous nanocellulose networks are impregnated by a solution of reactive hyperbranched polymers which is then subjected to thermal cross-linking. A hydroxyl-

functional hyperbranched aliphatic polyester in methanol solution is used with a melamine-based curing agent (HMMM) [20]. The preparation procedure involves solvent exchange of a nanocellulose hydrogel followed by polymer solution impregnation [21]. This procedure offers great potential in that many different solvents are feasible and a range of polymers can be used, yet the potential advantages of a tough nanopaper structure are preserved.

Experiments and methods

Materials

The cellulose nanofibers are microfibrillated cellulose, MFC, provided by Innventia AB. MFC was prepared from enzymatically pretreated bleached sulphite softwood pulp (Domsjö ECO Bright) by microfibrillation in a Microfluidizer, Microfluidics M-110EH, Microfluidics Inc [11]. Hyperbranched polymer Boltorn H30 was supplied by Perstorp Specialty Chemicals AB, and hexamethoxymethyl melamine (HMMM) by Becker Industrial Coatings AB, and TONE polyol 0301 was from Union Carbide. Texanol (2,2,4-trimethyl-1,3-pentanediol monoisobutyrate) and methanol were purchased from Sigma-Aldrich.

Preparation of MFC nanofiber films

0.4 g (dry weight) of MFC dispersion was diluted to 0.2 wt.-% and stirred for 48 h. Films of cellulose nanofibers were prepared by filtration. A glass filter funnel (7.2 cm in diameter) was used with a filter membrane, 0.65 μm DVPP, Millipore. The wet film was placed between two metal plates and dried at 55 °C for 48 h. The resulting thickness varied in the range of 60-70 μm between the prepared films.

Preparation of polymer matrix films

Boltorn H30 (3.25 g, 65 wt.-% of the dry weight) was added to a round-bottomed flask and preheated in an oven at 140 °C until it melted. The flask was put in an oil bath at 60 °C and methanol (3.0 g) was added. The mixture was stirred. HMMM (0.75 g, 15 wt.-% of the dry weight) and TONE polyol 0301 (1.0 g, 20 wt.-% of the dry weight) were added and dissolved. A film-forming additive, Texanol, was added. Films were applied to Teflon substrates with a 200 µm frame applicator. The solvent was evaporated at room temperature for 2 hours and then at 50 °C over night. Subsequently, the films were cured at 140 °C for 20 minutes, and the resulting thicknesses were 40-60 µm.

Preparation of composites

Matrix solutions were prepared by adding Boltorn H30 (9.75 g) to a round-bottomed flask and preheated in an oven at 140 °C until it melted. Methanol was added (135 mL, 85 mL and 50 mL for the 10 w/v%, 15 w/v%, and 30 w/v% matrix solution) and the flask was heated to 60 °C, and stirred. HMMM (2.25 g) and TONE polyol 0301 (3 g) were added.

The filtered, wet cellulose nanofiber hydrogel films were subjected to solvent exchange where water was replaced by methanol. These films were then immersed in 30 ml of the matrix solution and kept in a vacuum desiccator for 24 h. The films were dried between metal plates at 55 °C for 24 h and then cross-linked at 140 °C and 10 MPa for 20 minutes. The nanofiber content was calculated from the final weight of the composite. The matrix solution concentrations were 30 w/v%, 15 w/v%, and 10 w/v% and resulted in composites with 33 wt.-%, 51 wt.-%, and 63 wt.-% cellulose nanofibers, respectively. This corresponds to volume fractions (V_f) of 0.26, 0.43 and 0.55, estimated from fiber weight fractions, measured density for the matrix=1090 kg/m³, assumptions of no porosity, and an estimated MFC density=1500 kg/m³. This estimation

was performed based on the fact that the degree of order, and subsequently the density, is expected to be lower for MFC than for the cellulose crystal which has a density of 1570 kg/m^3 [22]. The composite film has a diameter of 70 mm and a thickness in the range of 80-230 μm , depending on composition.

Field emission scanning electron microscopy, FE-SEM

The microstructure of the composites was studied with S-4800 scanning electron microscope. The specimens were coated by gold using an Agar HR sputter coater. The surfaces of the composites and the fracture surfaces were analyzed at 2 kV acceleration voltage.

Density and porosity

An Archimedes scale was used for determination of density of the matrix and the cellulose nanofiber film. The density was calculated from sample displacement when immersed in mercury [23]. The porosity was calculated assuming a cellulose density of 1500 kg/m^3 .

Tensile testing

Tensile tests of the films were performed with an Instron machine equipped with a 100 N or a 500 N load cell. Specimens were 5 mm wide and thicknesses were uniform and 50-230 μm depending on composition. Grip distance was 20 mm and testing was performed at a cross-head speed of 2 mm/min. Specimens were conditioned and tested at 50% relative humidity and 23 °C. Displacement was measured by Differential Speckle Photography (DSP) [24]. A pattern was prepared for the DSP by printer toner. Data are based on at least 5 specimens. The toughness is defined as work-to-fracture, calculated from the area under the stress-strain curve.

Dynamic mechanical analysis, DMA

The DMA data were obtained with a TA Instruments Q800 in tensile mode. The grip distance was 10 mm and the heating rate was 2 °C min⁻¹. The specimens, 5 mm wide and with a thickness varying between 50 μm and 230 μm, were dried in a vacuum oven at 50 °C prior to analysis.

Estimate of interfiber distance and volume fraction modified matrix

The interfiber distance, s , is calculated according to equation (1) assuming continuous, unidirectionally oriented fibers and hexagonal packing [25]. The real material consists of flexible nanofibers oriented random-in-the-plane, so the real distances have a wide distribution but the scale is the same. V_f is the fiber volume fraction and r is the fiber radius.

$$s = 2 \left[\left(\frac{\pi}{2\sqrt{3}V_f} \right)^{\frac{1}{2}} - 1 \right] r \quad (1)$$

The ratio of the volume fraction of modified matrix, V_{mm} , to the total volume fraction matrix, V_m , where $V_m = 1 - V_f$, is calculated from equation (2) [25].

$$\frac{V_{mm}}{V_m} = \frac{t(2r+t)}{r^2} \left(\frac{1}{V_m} - 1 \right) \quad (2)$$

Results and discussion

Structure

Images of the composites with a nanofiber volume fraction of 0.26 content, and porous neat cellulose “nanopaper” structures are presented in Figure 1. The surface of cellulose nanopaper reveals a fibrous structure, where the cellulose nanofibers are randomly distributed, see Figure 1a. The cross-section shows a layered structure, see Figure 1b. The porosity of the nanopaper is 24%, based on density data (1140 kg/m³). The FE-

SEM images show a random-in-plane fiber distribution rather than random-in-space. This is confirmed by x-ray diffraction [14].

The porous cellulose nanofiber film is observed to absorb the uncured liquid matrix during impregnation and the nanofiber orientation distribution within the composites should therefore be similar to the nanofiber film with 100% cellulose. The composites surfaces are more featureless due to the presence of polymer matrix. The layered structure of the cross section can still be observed in the composites, see Figure 1c. The porosity is reduced, due to the addition of matrix as well as the hot-pressing. Careful scrutiny still makes it possible to discern some porosity in the nanocomposite samples.

Mechanical properties

Free-standing specimens of the nanocomposite films were characterized by dynamic mechanical analysis (DMA) in tensile mode. As can be seen in Figure 2a, the storage modulus increased significantly with increased amount of cellulose nanofibers in the films, especially in the rubbery region above T_g . There is a large difference between the pure polymer matrix and the nanocomposite film with a nanofiber volume fraction of $V_f=0.26$. The storage modulus for cellulose $V_f=0.43$, 0.55 and 1 increases in the anticipated order.

The peak in the $\tan \delta$ curve, see Figure 2b, represents the matrix T_g . For the polymer matrix reference sample, the glass transition occurs at 48 °C. The curve for the film with cellulose nanofiber $V_f=0.26$ exhibits two peaks, so the matrix has two T_g 's, at 48 °C and 92 °C. The latter could be due to a matrix phase chemically linked with nanofiber surfaces. Another contributing factor could be physically bound regions of polymer in the vicinity of the nanosized particles, in which the mobility of the polymer chains is strongly affected [26]. In the curve for the film with cellulose $V_f=0.43$ the

lower T_g peak at 48 °C is still visible, but much smaller. The dominant second T_g is in this curve slightly shifted upwards to 94 °C. At a cellulose nanofiber $V_f=0.55$, the material no longer exhibits two T_g 's and the remaining T_g is now shifted all the way up to 119 °C. This is an increase of more than 70 °C, which is quite remarkable. The fact that the original $\tan \delta$ peak for the matrix reference is lowered and widened in the nanocomposite curves is interesting. The decrease in peak height indicates a matrix structure with increased physical and chemical cross-links while the widening of the peak indicates an increased distribution of effective average molar mass between the physical and chemical cross-links. This is expected if a substantial fraction of the matrix is interacting with the nanofiber surfaces in the network.

It is useful to consider the approximate scale of the interfiber distances in these materials. We can for simplicity assume that all nanofibers have a diameter of 20 nm, are cylindrical, and oriented in the same direction. A certain matrix region close to the fiber surface is altered, and the thickness of this region is t . The shortest distance between nanofiber surfaces for the case of hexagonal fiber packing is denoted s , see Table 1. The thickness t is selected on the basis of an estimated diameter of the hyperbranched molecule of 3 nm, based on information in the literature [27].

Considering data for a 3 nm thick interphase region, the estimation of affected matrix fraction V_{mm}/V_m becomes as large as 24-84%. In order to put this into perspective the interfiber distance s and affected matrix fraction is also presented for fibers with 20 μm diameter. The nanoscale effect is substantial.

The Young's modulus and strength increase dramatically with increasing nanofiber content compared with the neat matrix (Figure 3, Table 2). The largest relative improvement in mechanical properties is observed for Young's modulus. The nanofiber composite with a volume fraction of 0.26 shows almost 900 times increase in

modulus compared with the neat matrix. The increase is even greater for the other composites. This is in agreement with the DMA results. The increase is due to the high modulus of the cellulose nanofiber network compared with the matrix material. The strength is also increased but more moderately. The great improvement in modulus and strength with addition of a cellulose nanofiber network is accompanied by decreased strain-to-failure.

Data for Young's modulus versus fiber content are presented in Figure 4a. Conventional composite micromechanics modeling predictions for materials with discrete fibers are not applicable due to the network reinforcement. In Figure 4b, the data for ultimate tensile strength are presented as a function of nanofiber content. At a volume fraction of 0.55, the average strength is 108 MPa. This is similar to data for a porous cellulose nanopaper structure without matrix and $V_f=0.62$ (106 MPa) [14]. It seems that the high- T_g matrix leads to premature failure at low strains. Interfiber-slippage mechanisms are likely to have a positive effect on strain-to-failure [14], and are hindered by the stiff matrix in this case.

Conclusions

A wood cellulose nanopaper template was impregnated by a hydroxyl-functional hyperbranched aliphatic polyester solution and polymerized to form a polymer network.

A strong increase in matrix T_g of up to 71 °C is observed for the nanocomposites containing up to 55% by volume of about 20 nm diameter nanofibers. The reason is decreased molecular mobility in the geometrically confined polymer network, due to interactions with the cellulose nanofiber surfaces. Covalent matrix-nanofiber linkages are present since HMMM can react chemically with hydroxyl groups at the nanofiber surfaces. This suggests a new nanocomposite concept where a significant proportion of

the confined polymer matrix is covalently attached to the cellulose nanofibers. Chemical stability is expected to be high in such materials since fiber-matrix interaction occurs through chemical bonding. The result also means that cellulose nanopaper templates are identified as a highly reactive reinforcement phase. This is a unique feature of cellulose nanopaper and contrasts with the properties of commonly used composites reinforcements such as polyethylene fibers, aramid fibers, carbon fibers, and carbon nanotubes.

Acknowledgements

Tom Lindström and Mikael Ankerfors, Innventia AB, Sweden, are acknowledged for kindly providing microfibrillated cellulose. The Swedish Research Council is gratefully acknowledged for financial support.

References

1. Sakurada I, Nukushina Y, Ito T. Experimental determination of the elastic modulus of crystalline regions in oriented polymers. *J Polym Sci* 1962;57:651-660.
2. Joffe R, Andersons J, Wallström L. Strength and adhesion characteristics of elementary flax fibres with different surface treatments. *Compos Part A – Appl S* 2003;34(7):603-612.
3. Favier V, Canova GR, Cavaille JY, Chanzy H, Dufresne A, Gauthier C. Nanocomposite materials from latex and cellulose whiskers. *Polym Adv Techn* 1995;6(5):351-355.
4. Favier V, Chanzy H, Cavaille JY. Polymer nanocomposites reinforced by cellulose whiskers. *Macromol* 1995;28(18):6365-6367.

5. Azizi Samir MAS, Alloin F, Dufresne A. Review of Recent Research into Cellulosic Whiskers, Their Properties and Their Application in Nanocomposite Field. *Biomacromol* 2005;6(2):612-626.
6. Berglund LA. Cellulose-based nanocomposites. In: Mohanty AK, Misra M, Drzal LT, editors. *Natural Fibers, Biopolymers, and their Biocomposites*; Boca Raton, Florida, USA: CRC Press, 2005.
7. Yano H, Sugiyama J, Nakagaito AN, Nogi M, Matsuura T, Hikita M, Handa K. Optically transparent composites reinforced with networks of bacterial nanofibers. *Adv Mater* 2005;17(2):153-155.
8. Shimazaki Y, Miyazaki Y, Takezawa Y, Nogi M, Abe K, Ifuku S, Yano H. Excellent Thermal Conductivity of Transparent Cellulose Nanofiber/Epoxy Resin Nanocomposites. *Biomacromol* 2007;8(9):2976-2978.
9. Iwamoto S, Nakagaito AN, Yano H, Nogi M. Optically transparent composites reinforced with plant fiber-based nanofibers. *Appl Phys A* 2005;81(6):1109-1112.
10. Henriksson M, Henriksson G, Berglund LA, Lindström T. An environmentally friendly method for enzyme-assisted preparation of microfibrillated cellulose (MFC) nanofibers. *Euro Polym J* 2007;43:3434-3441.
11. Pääkkö M, Ankerfors M, Kosonen H, Nykänen A, Ahola S, Österberg M, Ruokolainen J, Laine J, Larsson PT, Ikkala O, Lindström T. Enzymatic Hydrolysis Combined with Mechanical Shearing and High-Pressure Homogenization for Nanoscale Cellulose Fibrils and Strong Gels. *Biomacromol* 2007;8(6):1934-1941.

12. M. Henriksson, L. A. Berglund, Structure and Properties of Cellulose Nanocomposite Films Containing Melamine Formaldehyde. *J Appl Polym Sci* 2007;106:2817-2824.
13. Svagan A, Azizi Samir MAS, Berglund LA. Biomimetic foams of high mechanical performance based on nanostructured cell walls reinforced by native cellulose nanofibrils. *Adv Mater* 2008;15(7):1263-1269.
14. Henriksson M, Berglund LA, Isaksson P, Nishino T. Cellulose Nanopaper Structures of High Toughness. *Biomacromol* 2008;9(6):1579-1585.
15. Svagan AJ, Azizi Samir MAS, Berglund LA. Biomimetic polysaccharide nanocomposites of high cellulose content and high toughness. *Biomacromol* 2007;8(8):2556- 2563.
16. Nakagaito AN, Yano H. Novel high-strength biocomposites based on microfibrillated cellulose having nano-order-unit web-like network structure. *Appl Phys A* 2005;80(1):155-159.
17. Hult A, Johansson M, Malmström E. Hyperbranched polymers. *Adv Polymer Sci* 1999;143:1-34.
18. Malmström E, Johansson M, Hult A, Hyperbranched aliphatic polyesters. *Macromol* 1995;28(5):1698-1703.
19. Magnusson H, Malmström E, Hult A, Johansson M. The effect of degree of branching on the rheological and thermal properties of hyperbranched aliphatic polyethers. *Polymer* 2001;43(2):301-306.
20. Fogelström L, Malmström E, Johansson M, Hult A. Hard and flexible coatings based on nanoparticle-filled hyperbranched polymers. Abstracts of Papers, 234th ACS National Meeting, Boston, MA, USA, August 19-23, 2007.

21. Nogi M, Ifuku S, Abe K, Handa K, Nakagaito AN, Yano H. Fiber-content dependency of the optical transparency and thermal expansion of bacterial nanofiber reinforced composites. *Appl Phys Letters* 2006;88(13):133124-133126.
22. [Ref] Preston RD, *The physical biology of plant cell walls*, Chapman and Hall, London, 1974, p. 134.
23. Baggerud E, Stenström S, Lindström T. Measurement of volume fractions of solid, liquid and gas in kraft and CTMP paper at varying moisture content. *International Paper Physics Conference Proceedings, Atlanta, Georgia, USA: TAPPI Press, 2003. p. 157-163.*
24. Ljungdahl J, Berglund LA, Burman M. Transverse anisotropy of compressive failure in European oak – a digital speckle photography study. *Holzforschung* 2006;60(2):190-195.
25. Hull D. *An Introduction to Composite Materials*, 1st edition, Cambridge Solid State Science Series, Cambridge: Cambridge University Press, 1993. p. 61-63.
26. Tsagaropoulos G, Eisenberg A. Dynamic Mechanical Study of the Factors Affecting the Two Glass Transition Behavior of Filled Polymers. Similarities and Differences with Random Ionomers *Macromol* 1995;28(18):6067-6077.
27. Ihre H, Anders H, Söderlind E. Synthesis, characterization, and ^1H NMR self-diffusion studies of dendritic aliphatic polyesters based on 2,2-bis(hydroxymethyl)propionic acid and 1,1,1-tris(hydroxyphenyl)ethane. *J Am Chem Soc* 1996;118(27):6388-6395.

Figure Captions

Figure 1. FE-SEM images of (a) film surface of 100% MFC, (b) fracture surface of 100% MFC, and (c) fracture surface of the composite with cellulose $V_f=0.26$. Scale bar in (a) is 1 μm and in (b-c) 2 μm .

Figure 2. DMA curve of nanocomposite films with $V_f=0$ (black), 0.26 (red), 0.43 (blue), 0.55 (green) and 1 (grey, dashed) cellulose nanofibers; (a) storage modulus, (b) $\tan \delta$.

Figure 3. Uniaxial stress-strain curves for cellulose nanocomposite films with $V_f=0$ (black), 0.26 (red), 0.43 (blue), 0.55 (green) and 1.0 (grey) cellulose nanofibers.

Figure 4. Young's modulus (a) and ultimate tensile strength (b) as a function of nanofiber content for cellulose nanocomposites with fiber volume fraction 0 to 1.0.

Tables**Table 1.** Effects of volume fraction nanofibers and fiber radius on the affected matrix fraction.

Volume fraction, V_f	Thickness, t [nm]	diameter=20 nm		diameter=20 μm	
		Interfiber distance, s^a [nm]	Affected matrix fraction, V_{mm}/V_m^b	Interfiber distance, s^a [nm]	Affected matrix fraction, V_{mm}/V_m^b
0.26	3.0	17.4	0.24	17400	0.00021
0.43	3.0	9.0	0.52	9000	0.00045
0.55	3.0	5.7	0.84	5700	0.00073

^a Calculated according to equation (1), ^b Calculated according to equation (2).

ACCEPTED MANUSCRIPT

Table 2. Mechanical properties for cellulose nanofiber reinforced nanocomposites from the uniaxial tensile test in figure 3. The samples are conditioned at 50% RH and 23 °C. The values in parentheses are the sample standard deviations.

Nanofiber volume fraction, V_f	Modulus [GPa]	Tensile strength [MPa]	Strain-to-failure [%]	Work to fracture [MJ/m^3]	Moisture content [%]
0	0.0036 (0.0007)	6.1 (1.5)	23.3 (3.8)	0.8 (0.3)	4.0
0.26	3.2 (0.5)	49.4 (4.8)	4.1 (1.2)	1.2 (0.3)	5.1
0.43	6.7 (0.9)	85.0 (10.3)	2.7 (0.2)	1.4 (0.1)	4.4
0.55	9.7 (1.6)	108 (17.7)	2.8 (0.3)	1.9 (0.4)	4.7
1.0	13.9 (1.1)	213 (14.9)	6.6 (0.7)	9.4 (1.5)	8.3

ACCEPTED MANUSCRIPT

Fig 1a

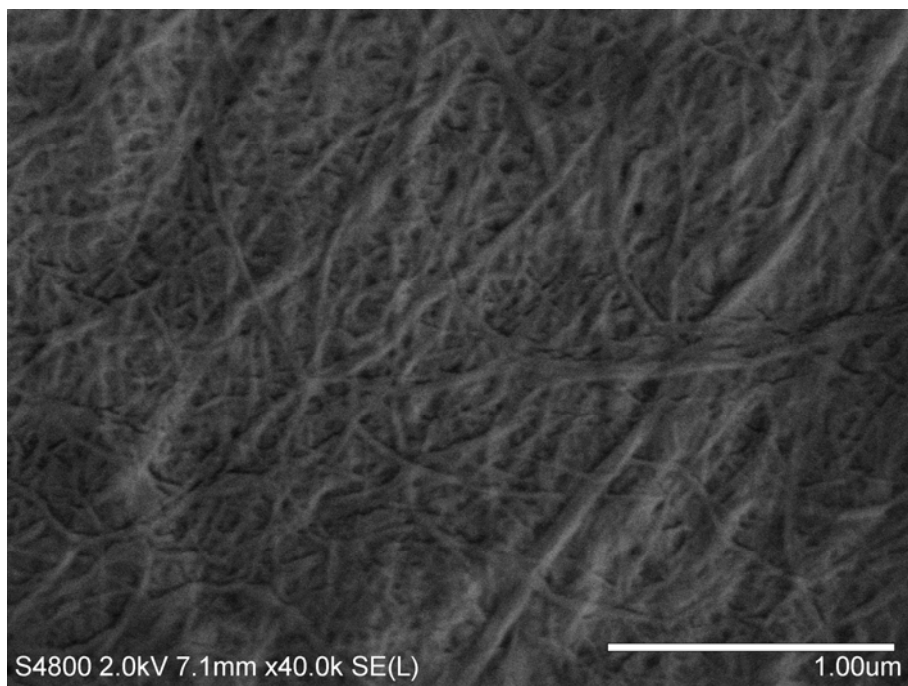


Fig 1b

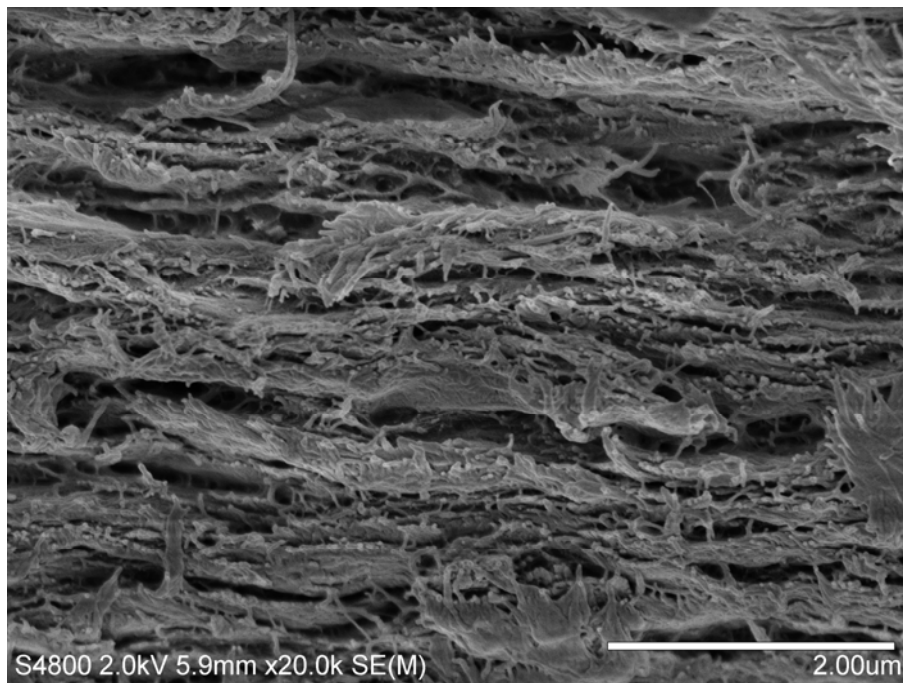


Fig 1c

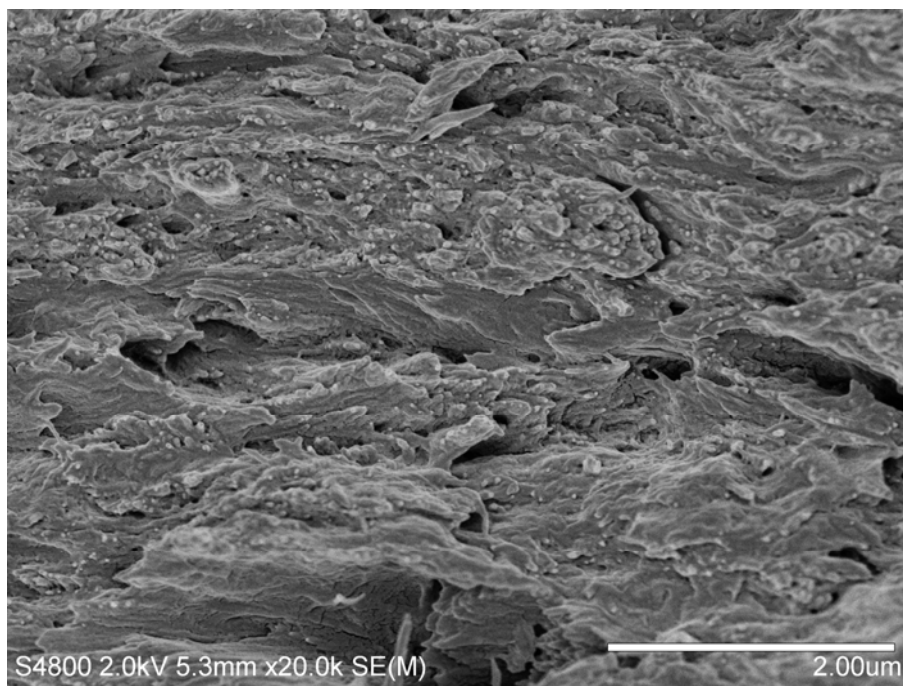
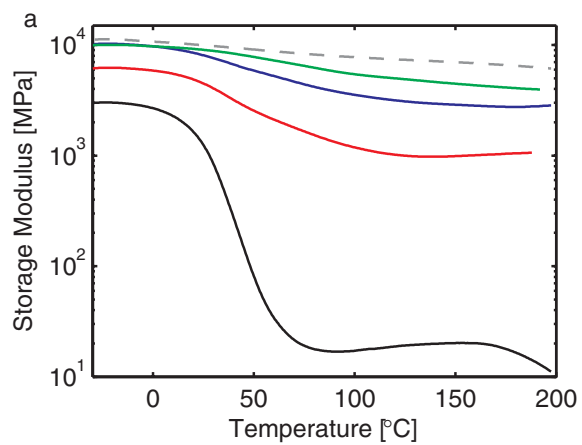
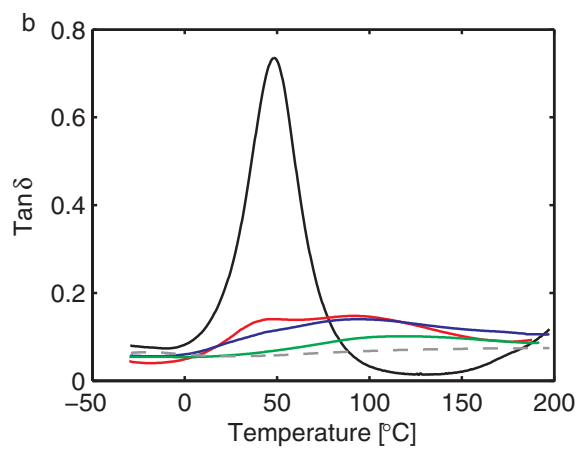


Fig 2a



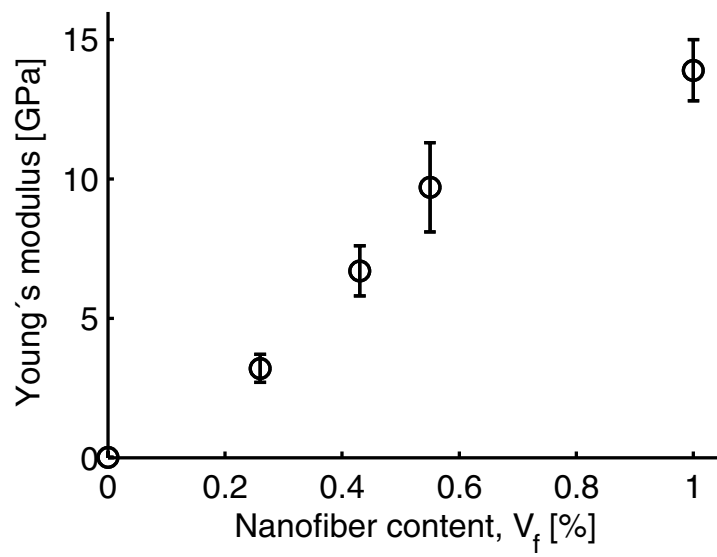
ACCEPTED MANUSCRIPT

Fig 2b



ACCEPTED MANUSCRIPT

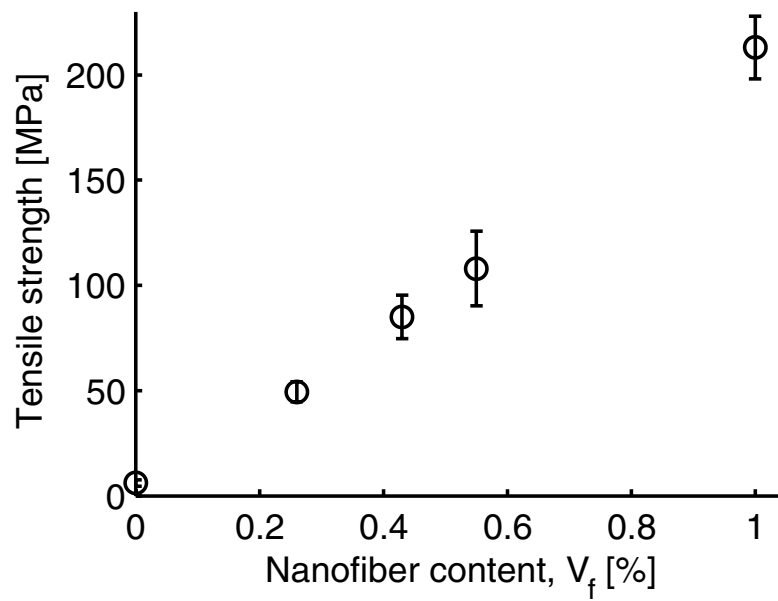
Fig 4a



ACCEPTED MANUSCRIPT

SCRIPT

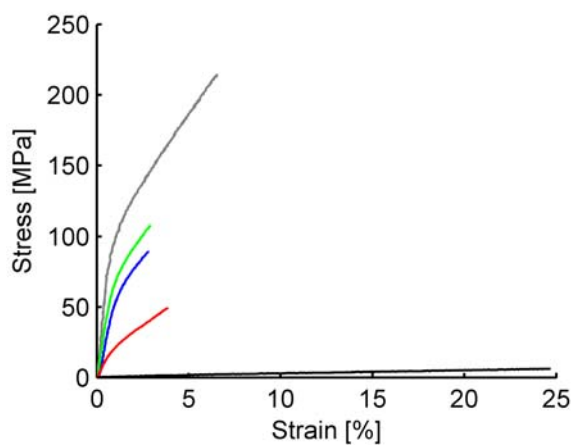
Fig 4b



ACCEPTED MANUSCRIPT

ACCEPTED MANUSCRIPT

Fig 3



ACCEPTED MANUSCRIPT